2014 IEEE International Conference on Robotics & Automation (ICRA)
Hong Kong Convention and Exhibition Center
May 31 - June 7, 2014. Hong Kong, China

Robot Assisted Gas Tomography - Localizing Methane Leaks in Outdoor Environments

Victor Hernandez Bennetts[1], Erik Schaffernicht[1], Todor Stoyanov[1], Achim J. Lilienthal[1] and Marco Trincavelli[1]

***Abstract*— In this paper we present an inspection robot to produce gas distribution maps and localize gas sources in large outdoor environments. The robot is equipped with a 3D laser range finder and a remote gas sensor that returns integral concentration measurements. We apply principles of tomography to create a spatial gas distribution model from integral gas concentration measurements. The gas distribution algorithm is framed as a convex optimization problem and it models the mean distribution and the fluctuations of gases. This is important since gas dispersion is not an static phenomenon and furthermore, areas of high fluctuation can be correlated with the location of an emitting source. We use a compact surface representation created from the measurements of the 3D laser range finder with a state of the art mapping algorithm to get a very accurate localization and estimation of the path of the laser beams. In addition, a conic model for the beam of the remote gas sensor is introduced. We observe a substantial improvement in the gas source localization capabilities over previous state-of-the-art in our evaluation carried out in an open field environment.**

I. INTRODUCTION

Detecting and localizing methane leaks is a relevant task for a variety of applications such as pipeline inspection [1], coal mine surveillance [2] and landfill monitoring [3]. Mobile robot olfaction, the sub-field of robotics, which develops robots with gas sensing capabilities, began its development in the early 1990s and until the early 2000s the gas sensitive robots were deployed in controlled mock-up environments [4]. Those robots were mostly trying to track an odour plume to the source using *in-situ* gas sensors (e.g. MOX sensors) and anemometers to sense the airflow [5]. More recently, other tasks for gas sensitive mobile robots like gas distribution mapping, leak localization, gas discrimination have been addressed. However, robots equipped with *in-situ* gas sensors need to enter the plume in order to detect and eventually identify the gas, which limits the applicability of gas sensing mobile robots. Recently, *remote* gas sensors based on Tunable Diode Absorption Spectroscopy (TDLAS) became commercially available. Some commercially available TDLAS devices can sense a specific gas (e.g. methane) up to a distance of 30 m without reflective mirrors. Remote gas sensors provide integral concentration measurements but no information about the distance travelled by the diode's beam or the gas distribution over the optical path.

The process of generating gas distribution maps from integral concentration measurements is referred to gas tomography [6]. Gas tomography requires, besides integral concentration measurements, information regarding the path travelled by the sensor's beam. In measurement configurations where the sensor is not fixed in a known position, the beam trajectory has to be estimated. Thus, gas tomography becomes heavily dependent on accurate ray tracing.

In this paper we present a robot equipped with a TDLAS and other sensing modalities that allow for accurate localization and beam tracing. We then use the localized beams to perform gas distribution modelling and the approach is evaluated in a large outdoor scenario. This work builds upon the results presented in [7] and improves them in many aspects. First, not only the map of the mean gas distribution is computed, but also a map of the variance (i.e. fluctuations) of the gas concentrations is built. The spatial distribution of the gas fluctuations can provide implicit information about the gas dispersion phenomenon. More specifically, areas of high concentration variance can be correlated to the proximity of a gas source [8]. Second, instead of using a coarse localization based on GPS data and odometry, a more precise system based on a 3D lidar and Normal Distributions Transforms (NDT) occupancy maps is employed. The improved localization accuracy allows for a much more accurate registration of the sensor readings in the maps, which results in better gas distribution models.

The paper is organized as follows. We will give an overview on remote gas sensing in general and its connection to robotics in Section II, before describing our robotic platform and the used sensors in Section III. Algorithms for performing robot localization, ray tracing and gas tomography are presented and discussed in Section IV. Section V describes the used experimental set up and results are reported in Section VI.

II. REMOTE GAS SENSING

Remote sensing emerged in the early 1990s when the development of new technologies allowed to measure gas concentrations without physically interacting with the target analytes. Remote sensors based on optical principles have gained momentum due to their high sensitivity, selectivity and stability [9].

A common principle in optical remote sensing is absorption spectroscopy, which measures the energy attenuation caused by molecules of a target gas at narrow bands of the electromagnetic spectrum. TDLAS sensors emit a laser beam tuned at the absorption band of the target gas. The laser diode

[1]AASS Research Centre, School of Science and Technology, Örebro University, Fakultetsgatan 1, Örebro, Sweden name.surname@oru.se

is modulated in a way that the emitted beam is driven on and off of the wavelength of interest. During this process, the power of the beam is measured continuously and, by comparing the measurements when the beam is on the target wavelength against the measurements when the beam is off, it is possible to determine, with high degree of selectivity, whether the emitted beam has traversed a target gas patch or not. Instead of providing a point measurement in *parts per million* (ppm), as in the case of *in-situ* sensing, remote sensors provide integral concentration measurement in *parts per million meters* ($ppm \cdot m$), with no information regarding the path followed by the beam or the distribution of the gas along the optical path.

Remote gas sensing can bring key benefits in the context of mobile robotics olfaction. Given that the robot does not need to physically travel to the location of a gas cloud to sample a measurement, larger exploration areas can be covered in shorter time and locations such as roofs and chimneys can be reached. In [10], a robot equipped with a TDLAS sensor was used to detect gas leaks in industrial environments using an ad-hoc triangulation algorithm. While the robot was able to travel towards the location of a leak, the performance of the algorithm heavily depended on the strong assumption that the detected concentration is located at the end of the beam. Grinham et al. [11] proposed a system to improve the quantification of CH_4 released rates from a water storage site. The authors mounted a *single-path* optical methane detector to an autonomous vessel and the collected data allowed the authors to identify areas of high CH_4 ebullition and predict release rates.

Computed Tomography for Gases (CTG) is the task of deriving gas distribution models from localized integral concentration measurements [6], [12]. CTG models can be either *pixel-based* or parametric. In the first approach, the model is given by a lattice in which, the concentration at each cell is estimated from a set of integral concentration measurements [13]. The latter approach, uses the integral measurements to fit the functional parameters of a set of n basis functions [14]. In this work, we present a *pixel-based* CTG algorithm.

While CTG has been proven feasible, a common approach is to use fixed sensing configurations, where the emitting diodes/reflectors are placed in predefined positions and therefore, the optical path of the beams are known. In the context of robots equipped with remote gas sensors, the estimation of the optical path is heavily determined by the accuracy of the robot's localization algorithm. The work presented in [7] is the first attempt towards robot assisted gas tomography.

III. THE ROBOTIC PLATFORM

The Gasbot prototype (originally introduced in [7]), shown in Fig. 1, is an all-terrain Husky A-200 robot equipped with different sensing modalities for robot localization and environmental monitoring. In this work, the TDLAS (Sewerin RMLD) sensor is used to measure CH_4, the 3D Lidar (Velodine $HDL-32E$) is used for localization purposes and the GPS unit (Xsens MTi-G) is used for evaluation purposes. No other sensing modalities are considered.

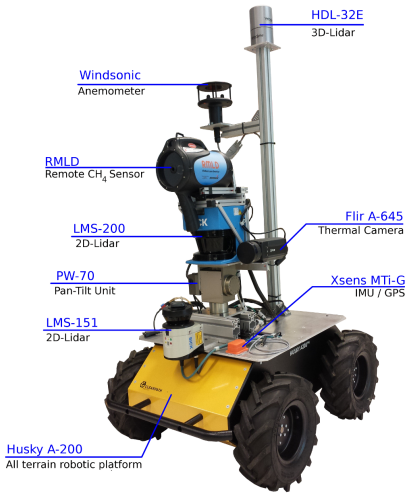

Fig. 1. Robotic platform "Gasbot". The sensors that are used in this paper are explained in the text.

The Remote Methane Leak Detector (RMLD) from Sewerin[1] can work in open loop with no mirrors required for reflection of the beam. According to the manufacturer's data sheets, the RMLD is able to measure CH_4 integral concentrations as low as 10 $ppm \cdot m$ at distances up to 30 m. Fig. 2 exemplifies the measurement principle of the RMLD. The sensor is mounted on top of a Pan-Tilt unit (PTU) PW-70, which allows to point the laser beam at different orientations, between $\pm 120°$ in the tilting axis and $360°$ in the panning axis. The $HDL-32E$[2] is a compact device that allows to generate point clouds of up to 700,000 points per second with a range of 100 meters and an accuracy of ± 0.02 m at 10 Hz.

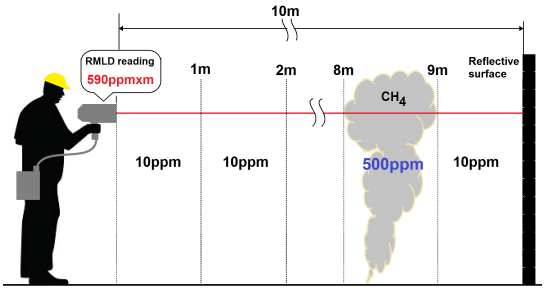

Fig. 2. Measurement principle of the RMLD. In the example, the device reports an integral concentration measurement of 590 $ppm \cdot m$ when the infra-red beams travels a 10 m path in which, a background concentration level of 10 ppm and a CH_4 patch of 500 ppm are present.

[1] http://www.sewerin.com/cms/en/products/gas/gas-leak-detection-outdoors/sewerin-rmld.html
[2] http://velodynelidar.com/lidar/hdlproducts/hdl32e.aspx

IV. ALGORITHMS

A. 3D Model Acquisition

A map of the environment is created using the recently proposed NDT fusion algorithm [15]. The NDT fusion algorithm is based on the Normal Distribution Transforms (NDT) framework and its Occupancy Map extension (NDT-OM, [16]). In the NDT framework, the exploration area is discretised and individual Gaussian probability density functions (pdf) are fitted using the measurement points that lie within the voxels in the lattice. Among different localization algorithms, NDT based approaches offer smooth likelihood models, that allow for very accurate localization [17].

The NDT fusion algorithm iterates between two steps. The track step of the algorithm performs an NDT-D2D registration [18] between the acquired range scan and the map. Once the tracking step has converged to a candidate pose, the new point cloud is inserted in the map using an efficient batch-update ray tracing procedure. The NDT fusion framework is applied directly to obtain consistent vehicle pose estimates and an incrementally constructed environmental map.

B. Ray Tracing

Tracing a ray through an NDT-OM map is a common operation, performed whenever new 3D range measurements are acquired. In this work however, ray tracing is also used to estimate the path associated with each measurement beam of the TDLAS sensor. The beam's starting point is estimated using the position and orientation of the gas sensor, relative to the robot's pose in the map. Then, a ray is traced from the start point through the map and the point of intersection is then obtained as the maximum likelihood point x_{ML} along the ray, given the Gaussian pdf in each traversed cell. If the likelihood is high enough, then the ray is likely to hit the distribution and x_{ML} is considered as the beam's endpoint.

C. Gas Distribution Mapping

The measurements of a Tunable Diode Laser Absorption Spectroscopy (TDLAS) sensor are line integrals of the gas concentration over the distance travelled by the beam. This scenario is similar to computer assisted tomography (CAT), where the image of a body of interest is reconstructed from a set of attenuation measurements of e.g. X-rays beams. The major difference is that bones are fixed while performing the CAT measurements, while gas disperses in the environment due to airflow advection and turbulence causing the gas distribution to be very dynamic. We will therefore estimate a model of the gas distribution that captures its statistical properties. We consider a polyhedral region that includes the volume for which the methane distribution map has to be produced. We divide the polyhedral region in a uniform grid of cubic cells. The purpose of the algorithm presented here is the estimation of the mean and variance of the methane concentration in each cell in the lattice from a set of TDLAS measurements. We start from the assumption that the statistics of the gas distribution (mean and variance) in each cell are constant over the duration of the experiments. No assumption is made about the spatial distribution of gases or

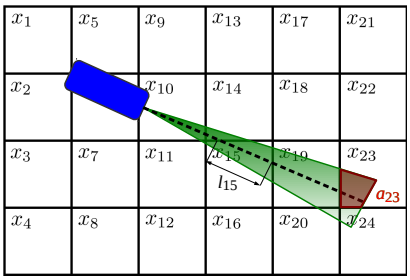

Fig. 3. Example scenario in which a measurement has been taken in an area described by a 4×6 lattice, with the sensor being placed in cell 10 and the laser being reflected on the ground in cell 23. Shown are the two different sensor models, line and cone. First, the dashed line represents the idealized beam model. It computes the length l the beam travels through each cell (depicted for cell 15). In this case, the measure obtained by the TDLAS sensor is $y_{beam} = l_{10}x_{10} + l_{14}x_{14} + l_{15}x_{15} + l_{19}x_{19} + l_{23}x_{23} + \epsilon$ where ϵ is the measurement noise. The second model is the more realistic cone model. The area of intersection a of the cone and each grid cell is computed, an example is shown in cell 23. The measurement is then expressed as $y_{cone} = a_{10}x_{10} + a_{11}x_{11} + a_{14}x_{14} + a_{15}x_{15} + a_{19}x_{19} + a_{20}x_{20} + a_{23}x_{23} + a_{24}x_{24} + \epsilon$.

the number of emitting sources present in the environment. In order to simplify the explanation, we consider a two dimensional example in Fig. 3.

As a further simplification, we will first consider that the measurement represents a line integral of the gas concentration over the path travelled by the beam. Therefore, we can write every measurement as:

$$y = \sum_{i=1}^{M} l_i x_i + \epsilon = \boldsymbol{l}^T \boldsymbol{x} + \epsilon \tag{1}$$

where y is the TDLAS reading, M is the number of cells, l_i is the distance travelled by the beam in cell i, x_i is the gas concentration in cell i, and ϵ is the measurement noise term. As a more realistic model of the real sensor , we model the laser as a cone instead of a beam. The cone is approximated by an isosceles triangle and we consider the area integral of the intersection of this triangle with the grid cell a_i instead of the line integral. Eq. 1 for the line model can again be used after substituting l with a in all cases.

In order to calculate the likelihood of the integral measurements, we assume Gaussian noise ϵ with zero mean and standard deviation σ:

$$p(y|\boldsymbol{x}, \boldsymbol{l}, \beta) = \mathcal{N}(y|\boldsymbol{l}^T\boldsymbol{x}, \sigma) \tag{2}$$

Now, having a set of N measurements, the problem of gas distribution mapping can be formulated as the problem to estimate the vector of concentrations x that maximizes the likelihood of the measurements. Given a set of N measurements, we can define a vector $\boldsymbol{y}[N \times 1]$ that contains all the measurement values, a vector $\boldsymbol{x}[M \times 1]$ that contains the concentration in the cells, and a matrix $\boldsymbol{L}[N \times M]$ that contains the line or area integral, respectively, that each measurement ray tracing produced. Therefore, the whole dataset of measurements can be described by the following matrix equation:

$$\boldsymbol{y} = \boldsymbol{L}\boldsymbol{x} + \epsilon\mathbf{1} \tag{3}$$

The likelihood of the measurements assuming Gaussian noise is:

$$p(\boldsymbol{y}|\boldsymbol{x}, \boldsymbol{L}, \beta) = \prod_{n=1}^{N} \mathcal{N}(y_n|\boldsymbol{L}\boldsymbol{x}, \sigma) \tag{4}$$

Maximizing the logarithm of the likelihood (equivalent to maximizing the likelihood itself) boils down to the following non negative least squares problem, which imposes the constraint $\boldsymbol{x} \succeq 0$, i.e. that gas concentrations have to be positive:

$$\begin{aligned} \underset{\boldsymbol{x}}{\text{minimize}} \quad & \|\boldsymbol{L}\boldsymbol{x} - \boldsymbol{y}\|_2^2 \\ \text{subject to} \quad & \boldsymbol{x} \succeq \mathbf{0} \end{aligned} \tag{5}$$

If some cells are never observed or many measurements are highly correlated the problem may become underdetermined and therefore it is useful to introduce a regularization term, modifying the problem in the following way:

$$\begin{aligned} \underset{\boldsymbol{x}}{\text{minimize}} \quad & \|\boldsymbol{L}\boldsymbol{x} - \boldsymbol{y}\|_2^2 + \lambda\|\boldsymbol{x}\|_2^2 \\ \text{subject to} \quad & \boldsymbol{x} \succeq \mathbf{0} \end{aligned} \tag{6}$$

which is analogous to choosing a Gaussian prior with zero mean on the average concentration of the cells. The strength of the prior is governed by the hyper-parameter λ. In our experiment we heuristically set $\lambda = 10^{-5}$, since we want to impose a weak prior. In our numerical results, we observe that the constraint $\boldsymbol{x} \succeq \mathbf{0}$ is never active, which implies that the obtained solution is the ordinary least squares solution $\hat{\boldsymbol{x}} = (\boldsymbol{L}^T\boldsymbol{L})^{-1}\boldsymbol{L}^T\boldsymbol{y}$. The case in which some entries of $\hat{\boldsymbol{x}}$ are equal to zero is of theoretical interest only and is not practically relevant. This estimator is unbiased which means that $E[\hat{\boldsymbol{x}}] = \boldsymbol{x}_*$, where $\boldsymbol{x}_*$ is the true value of the mean concentration in the cells. The covariance matrix of the estimator is:

$$cov(\hat{\boldsymbol{x}}) = E[(\hat{\boldsymbol{x}} - \boldsymbol{x}_*)(\hat{\boldsymbol{x}} - \boldsymbol{x}_*)^T] = \tag{7}$$

$$= (\boldsymbol{L}^T\boldsymbol{L})^{-1}\boldsymbol{L}^T E[\epsilon\epsilon^T]\boldsymbol{L}(\boldsymbol{L}^T\boldsymbol{L})^{-1} = \tag{8}$$

$$= (\boldsymbol{L}^T\boldsymbol{L})^{-1}\boldsymbol{L}^T(\sigma^2\boldsymbol{I})\boldsymbol{L}(\boldsymbol{L}^T\boldsymbol{L})^{-1} = \sigma^2(\boldsymbol{L}^T\boldsymbol{L})^{-1} \tag{9}$$

The diagonal elements of the covariance matrix are the variance of the estimators of the individual parameters, i.e. the variance of the gas concentration in each cell. We are left with the estimation of the variance of the process noise σ^2. If we call the vector of residuals $\boldsymbol{r} = \boldsymbol{y} - \boldsymbol{L}\hat{\boldsymbol{x}}$, the variance of $\boldsymbol{r}$ is:

$$var(\boldsymbol{r}) = E[\boldsymbol{r}^T\boldsymbol{r}] = E[tr(\boldsymbol{r}\boldsymbol{r}^T)] = tr(E[\boldsymbol{r}\boldsymbol{r}^T]) = \tag{10}$$

$$= tr(E[\boldsymbol{M}\epsilon\mathbf{1}\epsilon\mathbf{1}^T\boldsymbol{M}^T]) = tr(\boldsymbol{M}E[\epsilon\mathbf{1}\epsilon\mathbf{1}^T]\boldsymbol{M}) = \tag{11}$$

$$= \sigma^2 tr(\boldsymbol{M}^2) = \sigma^2 tr(\boldsymbol{M}) = \sigma^2(N - M) \tag{12}$$

Fig. 4. (a) The Gasbot platform patrolling the experimental area. (b) Artificial CH_4 gas source.

where $\boldsymbol{M} = \boldsymbol{I} - \boldsymbol{L}(\boldsymbol{L}^T\boldsymbol{L})^{-1}\boldsymbol{L}^T$ is a symmetric and idempotent matrix. An unbiased estimator of σ^2 is:

$$s^2 = \frac{\boldsymbol{r}^T\boldsymbol{r}}{N - M} \tag{13}$$

For more detailed explanations on the derivations of the formula the interested reader can consult [19].

V. EXPERIMENTAL SETUP

Experiments were conducted near the Örebro University's main campus (Fig. 4(a)), where an artificial gas source was placed. The gas source was a flask of natural gas ($\sim 90\%$ CH_4) connected to a tube ring punctured in multiple places. In order to diffuse the *jet-like* emissions coming from the punctures, a permeable mat was used to cover the ring (4(b)). During the experimental trials, the ambient temperature was 16° C with a moderate wind flow of 1.6 m/s.

Two experiments were carried out in which the robot was remotely commanded to follow different exploration paths inside areas of approximately 154 m^2 and 432 m^2 respectively. The total exploration time was approximately 1200 s in both cases. During the exploration, the robot was stopping to collect gas measurements. At each stop position, the PTU was used to scan the neighbouring area in a continuous sweeping movement with apertures of $(-70^\circ, 70^\circ)$ and $(-8^\circ, -2^\circ)$ in pan and tilt respectively. The RMLD was always pointing towards the ground (grass surface), which was used as reflective surface. No artificial reflectors were introduced in the experimental location.

VI. RESULTS

Since accurate ground truth on the real gas distribution is, with currently available instrumentation, impossible to acquire in generic uncontrolled environments like the presented experimental setup, we evaluate the gas distribution models according to their capability to predict the location of the gas source. In [7], bottles filled with methane were successfully localized using the maximum of the mean concentration map as an indicator. Here we show that in real world scenarios, where methane is dispersed in the environment from a leaking gas source and not confined into static volumes, the maximum of the concentration variance map, one of the novelties proposed in this paper, is a much better indicator of the position of the gas source. Fig. 5 shows example maps

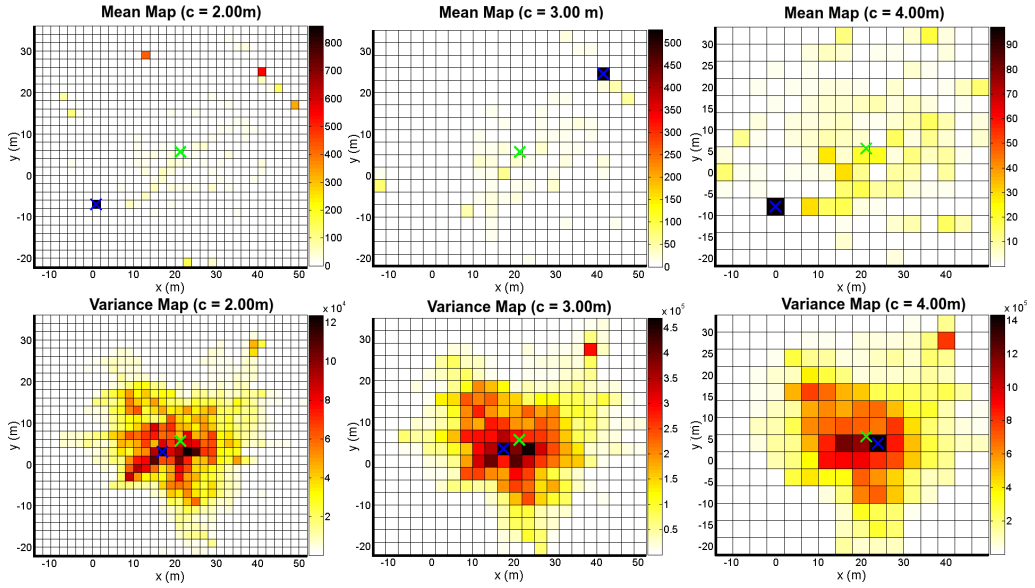

Fig. 5. Mean and variance of the gas distribution for various map resolutions. The green marker indicates the true position of the gas source, while the blue marker indicates the estimated position of the gas source (maximum of the mean/variance map).

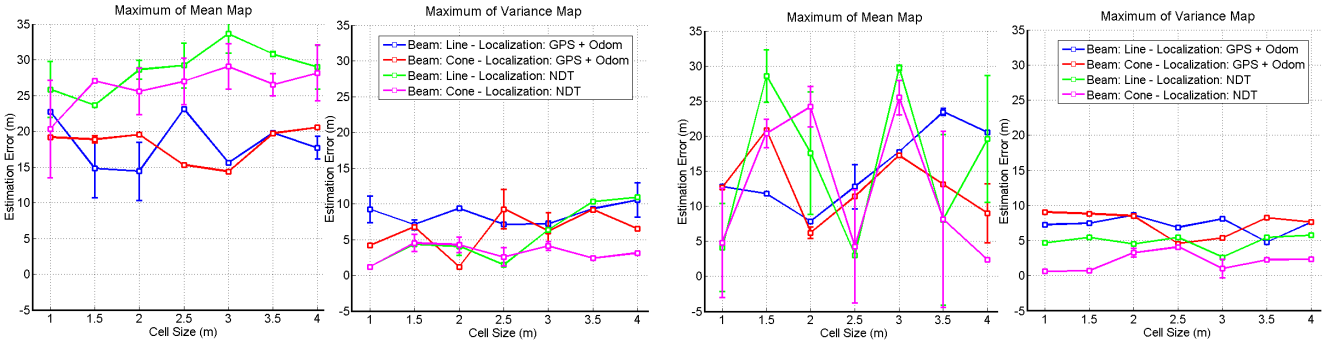

(a) (b)

Fig. 6. Gas source localization accuracy. (a) First experimental run (explored area 154 m^2). (b) Second experimental run (explored area 432 m^2).

obtained for various cell sizes in one of our experimental runs. In order to numerically evaluate the improvements introduced by the NDT based localization and the conic beam model we divide the two datasets into 5 folds each and calculate errorbars for the accuracy of the gas source position estimation. Figure 6(a) and 6(b) show the results for the two experimental runs. From the distances between the real and estimated gas source position, it is clear that the maximum of the variance map (errors consistently below $10m$) provides a better indicator of the gas source position than the maximum of the mean map (errors between $25m$ and $35m$). Focusing the attention on the predictions obtained with the variance map, we can see how in general the positioning and ray tracing obtained with the NDT model (errors in the order of $2m - 4m$) outperform the positioning based on filtered GPS and odometry (errors around $10m$) presented in [7]. Regarding the comparison of the beam models, we can see how the models obtained with the conical beam model (errors between $1m$ and $4m$) clearly outperform the models based on the line beam model in the second experimental run, while in the first experimental run, a clear difference is visible only for cell sizes $\geq 3m$.

VII. CONCLUSIONS

In this paper we present an approach for robot assisted gas tomography. The contributions of this paper, which builds upon the work presented in [7], are three-fold. First a state-of-the-art NDT-OM localization system, which uses the input from a 3D LIDAR and the odometry of the robot, is used for accurately localizing the beams of the TDLAS sensor. This results in higher quality gas distribution maps. We improved a previously proposed gas distribution mapping algorithm so that it estimates not only the mean but also of the variance of gas concentration. Third, a more realistic conic shaped sensor model is proposed instead of the previously used line model. It is worth noting that the proposed system has been evaluated on a large experimental area similar to the one where fully fledged gas inspection robots could be deployed (e.g. a decommissioned landfill). While no ground truth evaluation could be performed performed with respect to

the predictive capabilities of the gas distribution models, we observed that the maximum of the variance map (computed with a conic model and with a more accurate 3D environment representation), is a much better indicator of the position of the gas source than the maximum of the mean map. This result is supported by previous work in which, measurements on turbulent underwater plumes show that the magnitude of the concentration fluctuations exhibit a steeper gradient along the downstream direction that the average concentration [20].

Several aspects require further investigation, which is deferred to future works. First, the performance of the gas distribution algorithm clearly depends on the choice of the cell size. A large cell size may lead to an oversimplified gas distribution model, while a small cell size may introduce estimation errors since the measurements cannot support such a complicated model. This particular instance of the well known bias-variance (model selection) dilemma may be solvable by a cross-validation approach similar to the one used for other gas distribution mapping algorithms like the Kernel DM+V (e.g. [21]).

Second, the choice of the location of the measurement clearly affects the quality of the model. The choice of the measurement points will most probably result from a trade-off between the desired quality of the model and the time needed to explore the whole area of interest.

Third, gas dispersion is a highly dynamic phenomenon and thus, the assumption of time invariant gas distribution models does not hold. This problem has been explored for *in-situ* gas sensors [22], [23] and a proposed solution is to consider the time stamps of the acquired concentration measurement in such a way that recent measurements are more significant when computing the gas distribution models.

Additional experiments are needed to thoroughly validate the proposed approach. These experiments should be carried out in locations other than open areas. For example, outdoor locations occluded by buildings/obstacles, uneven terrains or urban locations. Furthermore, a grid of *in-situ* gas sensors could be added to provide ground truth concentration measurements for evaluation purposes.

ACKNOWLEDGMENTS

The authors would like to thank Robotdalen, for funding this work as part of the Gasbot project (project number 8140), and Clearpath Robotics, for providing the Husky A-200 robotic platform through its PartnerBot program.

REFERENCES

[1] R. A. Alvarez, S. W. Pacala, J. J. Winebrake, W. L. Chameides, and S. P. Hamburg, "Greater focus needed on methane leakage from natural gas infrastructure," *Proceedings of the National Academy of Sciences*, vol. 109, no. 17, pp. 6435–6440, 2012.

[2] M. A. Meybodi and M. Behnia, "Australian coal mine methane emissions mitigation potential using a stirling engine-based chp system," *Energy Policy*, vol. 62, no. 0, pp. 10 – 18, 2013.

[3] V. Hernandez Bennetts, A. J. Lilienthal, P. Neumann, and M. Trincavelli, "Mobile robots for localizing gas emission sources on landfill sites: Is bio-inspiration the way to go?" *Frontiers in Neuroengineering*, vol. 4, no. 20, 2012.

[4] G. Kowadlo and R. A. Russell, "Robot Odor Localization: A Taxonomy and Survey," *The International Journal of Robotics Research*, vol. 27, no. 8, pp. 869 – 894, 2008.

[5] A. J. Lilienthal, A. Loutfi, and T. Duckett, "Airborne chemical sensing with mobile robots," *Sensors*, vol. 6, no. 11, pp. 1616–1678, 2006.

[6] P. Price, M. Fischer, A. Gadgil, and R. Sextro, "An algorithm for real-time tomography of gas concentrations, using prior information about spatial derivatives," *Atmospheric Environment*, vol. 35, no. 16, pp. 2827–2835, 2001.

[7] V. Hernandez Bennetts, A. Lilienthal, A. A. Khaliq, V. Pomareda Sese, and M. Trincavelli, "Towards real-world gas distribution mapping and leak localization using a mobile robot with 3d and remote gas sensing capabilities," in *Proceedings of the IEEE International Conference on Robotics and Automation (ICRA)*, 2013, pp. 2327–2332.

[8] S. Asadi, M. Reggente, C. Stachniss, C. Plagemann, and A. J. Lilienthal, *Intelligent Systems for Machine Olfaction: Tools and Methodologies*. IGI Global, 2011.

[9] X. Liu, S. Cheng, H. Liu, S. Hu, D. Zhang, and H. Ning, "A survey on gas sensing technology," *Sensors*, vol. 12, no. 7, pp. 9635–9665, 2012.

[10] G. Bonow and A. Kroll, "Gas leak localization in industrial environments using a tdlas-based remote gas sensor and autonomous mobile robot with the tri-max method," in *Robotics and Automation (ICRA), 2013 IEEE International Conference on*, May 2013, pp. 987–992.

[11] A. Grinham, M. Dunbabin, D. Gale, and J. Udy, "Quantification of ebullitive and diffusive methane release to atmosphere from a water storage," *Atmospheric Environment*, vol. 45, no. 39, pp. 7166 – 7173, 2011.

[12] R. Byer, "Two-dimensional remote air-pollution monitoring via tomography," *Optics Letters*, vol. 4, no. 3, pp. 75–77, 1979.

[13] M. Trincavelli, V. Bennetts, and A. Lilienthal, "A least squares approach for learning gas distribution maps from a set of integral gas concentration measurements obtained with a tdlas sensor," in *Sensors, 2012 IEEE*, Oct 2012, pp. 1–4.

[14] A. Drescher, A. Gadgil, P. Price, and W. Nazaroff, "Novel approach for tomographic reconstruction of gas concentration distributions in air: Use of smooth basis functions and simulated annealing," *Atmospheric Environment*, vol. 30, no. 6, pp. 929–940, 1996.

[15] T. Stoyanov, J. Saarinen, H. Andreasson, and A. Lilienthal, "Normal distributions transform occupancy map fusion: Simultaneous mapping and tracking in large scale dynamic environments," in *Intelligent Robots and Systems (IROS), 2013 IEEE/RSJ International Conference on*, Nov 2013, pp. 4702–4708.

[16] J. Saarinen, H. Andreasson, T. Stoyanov, J. Ala-Luhtala, and A. Lilienthal, "Normal distributions transform occupancy maps: Application to large-scale online 3d mapping," in *Robotics and Automation (ICRA), 2013 IEEE International Conference on*, May 2013, pp. 2233–2238.

[17] J. Saarinen, H. Andreasson, T. Stoyanov, and A. Lilienthal, "Normal distributions transform monte-carlo localization (ndt-mcl)," in *Intelligent Robots and Systems (IROS), 2013 IEEE/RSJ International Conference on*, Nov 2013, pp. 382–389.

[18] T. Stoyanov, M. Magnusson, and A. J. Lilienthal, "Fast and accurate scan registration through minimization of the distance between compact 3d ndt representations," *The International Journal of Robotics Research*, vol. 31, pp. 1377–1393, 2012.

[19] C. Heij, P. de Boer, P. H. Franses, T. Kloek, and H. K. van Dijk, *Econometric Methods with Applications in Business and Economics*. Oxford University Press, 2004.

[20] D. Webster, S. Rahman, and L. Dasi, "Laser-induced fluorescence measurements of a turbulent plume," *Journal of Engineering Mechanics*, vol. 129, no. 10, pp. 1130–1137, 2003.

[21] A. J. Lilienthal, M. Reggente, M. Trincavelli, J. L. Blanco, and J. Gonzalez, "A statistical approach to gas distribution modelling with mobile robots the kernel dm+v algorithm," in *Proceedings of the IEEE/RSJ International Conference on Intelligent Robots and Systems (IROS)*, October 11 - October 15 2009, pp. 570–576.

[22] J. G. Monroy, "Advances in gas sensing and mapping for mobile robotics," Ph.D. dissertation, University of Malaga, nov 2013.

[23] S. Asadi, S. Pashami, A. Loutfi, and A. J. Lilienthal, "Td kernel dm+v: Time-dependent statistical gas distribution modelling on simulated measurements," in *AIP Conference Proceedings Volume 1362: Olfaction and Electronic Nose - Proceedings of the 14th International Symposium on Olfaction and Electronic Nose (ISOEN)*, 2011, pp. 281–283.